Charge-state transitions of muonium in germanium

R. L. Lichti

Department of Physics, Texas Tech University, Lubbock, Texas 79409-1051

S. F. J. Cox

ISIS Facility, Rutherford Appleton Laboratory, Chilton, OX11 0QX, United Kingdom
and Department of Physics, University College London, London WCE 6BT, United Kingdom

K. H. Chow

Department of Physics, Lehigh University, Bethlehem, Pennsylvania 18015-3039

E. A. Davis

Department of Physics, University of Leicester, Leicester LEI 7RH, United Kingdom

T. L. Estle

Department of Physics, Rice University, Houston, Texas 77251-1892

B. Hitti

TRIUMF, 4004 Wesbrook Mall, Vancouver, Canada V6T 2A3

E. Mytilineou

Department of Physics, University of Patras, Patra, Greece

C. Schwab

PHASE, Centre National de la Recherche Scientifique, 67037 Strasbourg, France

(Received 11 December 1998)

Muonium defect centers in ultrapure germanium show evidence of cyclic charge-state transitions above approximately 220 K. Detailed analysis of the magnetic-field and temperature dependences of longitudinal muon spin depolarization rates reveals contributions from both bond-centered and tetrahedral cage-centered interstitial Mu^0 species involved in separate ionization/capture charge cycles. An additional diamagnetic state, observed as a nonrelaxing fraction, is identified as muonium bound in a slowly formed complex which dissociates to join these cycles above 350 K. Capture cross sections and ionization energies are extracted and the most likely identification of states and processes responsible for each transition feature are discussed. A consistent picture requires a reinterpretation of earlier data as bidirectional site changes for Mu^0 which become active well below 100 K, and indicates a very shallow potential-energy surface for Mu^0 in germanium as compared to silicon. [S0163-1829(99)04627-5]

I. INTRODUCTION

Hydrogen enters many semiconductor materials during crystal growth or in device processing steps, typically forming bound complexes with intentional dopants and other defects, and thereby modifying the electrical activity. The effectiveness of these ''passivation'' reactions depends to a significant extent on the mobility and charge state of the isolated hydrogen defect centers. However, except for a few measurements in silicon, there is very little direct experimental information regarding the individual isolated hydrogen states, and most reported properties are inferred indirectly with assumptions as to which hydrogen center or centers may be present. Fortunately, data on the light pseudoisotope of hydrogen known as muonium ($Mu=[\mu^+, e^-]$), which is formed when an implanted positive muon captures an electron, have provided a vast wealth of detailed experimental results on a closely analogous system.[1–3] Where data exist

for both H and Mu centers, their static properties are extremely well correlated.[3] We have recently been investigating the dynamics of Mu diffusion and transitions among the various Mu states, concentrating mostly on Si and GaAs.[4–8] Results of these studies clearly demonstrate that Mu (and by inference H) undergoes a series of very rapid transitions above room temperature involving several charge states and structural configurations. These data have yielded significant information on the atomic-level interactions related to hydrogen diffusion processes, and have provided hints as to why hydrogen passivation occurs more readily under certain conditions than in others.

The relatively complex behavior of muonium in semiconductors is probably best understood in silicon, which is certainly the most extensively studied case. Muonium forms four distinct interstitial defect states or centers in the diamond-structured materials. Two of these have the muon centered in a stretched host bond. Based primarily on theo-

retical considerations,[9] this bond-centered (BC) configuration is the ground state for neutral muonium in Si and is the stable site for the positively charged center. We label these two states as Mu_{BC}^0 and Mu_{BC}^+, respectively. For the other two centers the muon resides within the largest interstitial cage region in the diamond structure, the center of which has tetrahedral symmetry. In silicon, this so-called T site is metastable for the neutral state and is the stable configuration for the negatively charged defect. These centers are denoted as Mu_T^0 and Mu_T^-, respectively. Although the local energy minimum for Mu_T may not be exactly at the cage center, rapid motion averages out any anisotropy. Of the neutral paramagnetic species, Mu_T^0 has a large and isotropic hyperfine interaction characteristic of the rather atomiclike nature of its electronic wave function. The wave function for Mu_{BC}^0 has a node at the muon location with the unpaired electron mostly on the two nearest-neighbor host atoms, resulting in a small $\langle 111 \rangle$-oriented highly anisotropic hyperfine interaction. As demonstrated most clearly in GaAs, the isotropic neutral Mu_T^0 hops or tunnels rapidly between T sites, and is far more mobile than any of the other muonium states.[10,11]

Even at quite low temperatures, numerous transitions occur on the time scale of the muon lifetime (2.199 μs): these include changes in the structural configuration, thermal ionizations, interactions with conduction electrons or holes, and perhaps interactions with other impurities. A total of eight separate processes leading to transitions among the four muonium states have been identified in silicon, with parameters governing the rate dynamics determined for each.[5,6] At high temperatures, above roughly 400 K for intrinsic Si, a rapid muonium charge-state cycle develops. Such a cycle can result from the alternating thermal ionization of Mu^0 and recapture of an electron from the conduction band, although a number of other possibilities also exist. Analysis of the depolarization data[4] for high-temperature Mu charge cycles in Si implies that the effective cycle involves $Mu_T^0 \rightleftharpoons Mu_{BC}^+$ transitions. Comparison of the relative rates[5] for transition paths out of the individual muonium states as extrapolated from measurements at lower temperatures, indicates that the relevant cycle in silicon involves three steps: (1) ionization of the Mu_{BC}^0 ground state; (2) an ''activated capture'' process in which the muon changes site, $Mu_{BC}^+ + e^- \rightarrow Mu_T^0$; and finally, (3) a $T \rightarrow BC$ configuration change for Mu^0 returning the system to its initial conditions. The largest activation energy in this transition cycle is for the electron-capture step into the mobile metastable Mu_T^0 state. Muonium charge cycles are seen in most of the semiconductors investigated thus far. However, except for Si, the only other semiconductor for which detailed information on the cycle has been reported[8] is metallic n-type GaAs where the high-temperature charge dynamics have been assigned to a $-/0$ cycle resulting from the alternating capture of electrons and holes by Mu_T. Similar charge cycles are expected to be active for muonium and hydrogen in the same materials since the *purely electronic* states and energies are nearly identical. With due allowance for different zero-point energies, the migrational kinetics of H and Mu should also be qualitatively similar. Based on the charge-cycle and diffusion results for muonium, we have concluded[12] that a highly mobile H_T^0 center should dominate hydrogen diffusion in Si and GaAs even

though it is not the thermodynamically favored state for isolated hydrogen in most circumstances.

The present investigation deals primarily with transitions found for Mu in an ultrapure sample of germanium. More specifically, we concentrate on analysis of the muonium charge cycles observed in muon spin depolarization[4,13] measured as the relaxation rate T_1^{-1} in a longitudinal magnetic field, i.e., applied parallel to the initial spin direction. Muonium forms the same type of defect centers in Ge as it does in Si, with the main difference being that theoretical calculations[14] predict that the two neutral species have nearly equal energies in Ge, with Mu_T^0 slightly lower. Arriving at a detailed understanding of the muonium transitions in Ge has been considerably more difficult than in Si, where features are well separated in temperature thus allowing the dynamics of individual transitions to be cleanly extracted. In early transverse-field muon spin rotation (TF-μSR) studies of Ge, the precession signals for Mu_T^0 and Mu_{BC}^0 were both found to disappear very near 100 K.[1] Temperature-dependent TF-μSR relaxation rates are reported to give Arrhenius energies of 12 and 26 meV, respectively, for transitions out of the two neutral states, with prefactors below 100 MHz.[1,15] All of these parameters are exceptionally low compared to values observed for thermal ionization processes of the Mu^0 centers in other semiconductors. The diamagnetic TF-μSR signal intensity, arising from charged Mu states, increases only above 150 K in Ge. This increase was analyzed in several n-type Ge samples as due to a $Mu_T^0 \rightarrow Mu^+$ transition where the parent state was subject to electron spin-flip scattering prior to ionization.[16] The resulting ionization energies fell within the range of 175 ± 10 meV, with prefactors near 10^7 MHz, in much better agreement with the ionization results in related materials. We previously published[13] preliminary low-field longitudinal depolarization data for Ge which show the onset of charge cycles near 220 K. A partial analysis of those data gave an ionization energy of 195 meV, assuming a $0/+$ cycle with an active Mu_T^0 neutral state and a temperature-independent electron-capture cross section. Those data display a second feature which could not be explained within the framework of a single two-state charge cycle, and which undoubtedly distorted the preliminary analysis.

We have now extended the longitudinal depolarization measurements on this sample to include both the temperature and magnetic-field dependences. A more complete analysis of the charge-cycle data and a re-examination of earlier data on Mu transition dynamics in Ge are presented here, expanding on a brief comparison of muonium dynamics in Ge and Si presented in recent conference proceedings.[17] While we are still not able to conclusively assign all of the individual transition processes, we discuss and evaluate the most likely options and obtain estimates of the transition rate parameters.

II. EXPERIMENTAL DETAILS

The germanium sample on which all of the data reported here were acquired is from an ultra-pure single crystal obtained from ORTEC. The original 75-mm-diameter wafer was 3 mm thick and oriented with the $\langle 100 \rangle$ crystallographic direction normal to the surface. The piece on which most data were obtained was cut to an octagonal shape with ap-

proximately 30-mm lateral dimensions. This Ge sample is slightly *p* type, with a net electrically active impurity concentration of 5.2×10^9 cm^{-3} as determined from Hall-effect and conductivity characterization. Based on information provided with the sample, other impurities are C at $\sim 10^{15}$ cm^{-3}, Si at $\sim 10^{13}$ cm^{-3}, O at 10^{12}–10^{13} cm^{-3}, and H at the 10^{15} cm^{-3} level initially. Extended periods at high temperatures under vacuum almost certainly drove off a significant fraction of the hydrogen during the course of these measurements.

The experiments were performed on the MuSR instrument of the ISIS Facility at the Rutherford Appleton Laboratory and on the M15 and M20b muon beamlines at TRIUMF. In each case the positive muon source was a $\simeq 100\%$ spin polarized ''surface'' beam with a momentum of ~ 29 MeV/c. The pulsed nature of the ISIS Facility limits accurate measurements of muon spin depolarization or relaxation rates to situations where rate constants are less than ~ 10 μs^{-1}, while a continuous source such as the TRIUMF cyclotron allows measurement of considerably faster rates. The primary data for this study were obtained in the longitudinal-field (LF) geometry in which an external magnetic field is applied parallel to the initial muon spin polarization direction.[2] The directly measured quantity is the asymmetry *A*, in the muon decay rates for positrons emitted along and opposite to the initial muon spin direction (the applied field direction) as determined by $A = (N_F - \alpha N_B)/(N_F + \alpha N_B)$. Here N_F and N_B represent the positron rates in detectors subtending a significant solid angle in the forward and reverse directions, respectively, and the balance factor α accounts for differences in detector efficiencies and geometrical acceptances. Since we are primarily interested in measuring the depolarization rates, we require the time dependence of the decay asymmetry $A(t)$. For a continuous source such as TRIUMF this is accomplished by restricting the incoming muon flux to $\leq 4 \times 10^4$ muons/s, so that only a single muon is allowed in the sample at any time, and keeping track of the time between implantation and decay. At a pulsed source such as ISIS, all muons in a single beam pulse (~ 200 muons) are admitted and all of the resulting decay events are placed in the appropriate time bins; however, the uncertainty of the implantation time (pulse width ~ 80-ns full width at half maximum) restricts measurement of high depolarization rates. In either case, each data point typically results from a histogram containing 5–20 million muon decay events depending on the depolarization rates to be measured and the accuracy demanded. These LF measurements are interspersed with normalization runs in a weak (2–8 mT) transverse field to determine α. This correction effectively fixes the $A = 0$ baseline in the low-field limit for the LF measurements. For fields above ~ 0.1 T the decay positron paths are significantly modified by the field, thereby changing the effective detector acceptances and thus α; therefore, the balance factor is adjusted at higher fields to values obtained under conditions where the full implanted muon fraction is known to rapidly depolarize, allowing a direct determination of the baseline. An accurate baseline is especially important when depolarization rates are small or when more than one component is present.

In the longitudinal geometry, the absence of spin precession means that separation of the signal intensity arising from different Mu states is based on analysis of multicomponent depolarization curves. In the transverse geometry a set of spin-precession frequencies are associated with a particular state. Vastly different hyperfine characteristics identify the two neutral paramagnetic centers.[1] On the other hand, the two diamagnetic charged centers Mu$^+$ and Mu$^-$ are nearly impossible to separate spectroscopically; thus, any assignment is based on different transition dynamics and on doping concentration and temperature dependences. In the longitudinal geometry, distinct field dependences for the hyperfine decoupling, or ''repolarization,'' curves $A_o(B_{LF})$ allow identification of components related to Mu$_{BC}^0$ and Mu$_T^0$.[1] Additionally, in the limit of slow spin- or charge-exchange rates, Mu$_{BC}^0$ can be identified as the active relaxing species from a characteristic peak in the field dependence of the depolarization rates.[18] The low-field TF-μSR data used for baseline normalizations also yield the total prompt *diamagnetic* signal intensity, which is ordinarily assigned to the sum of the two charged Mu states.

In longitudinal fields which are large enough to decouple the static local fields due to nuclear moments, any relaxation of the asymmetry is the result of dynamic processes such as muonium state transitions or muon motion. These consequently lead to exponential relaxation functions: they are true depolarization (T_1) processes due to fluctuations in a relevant magnetic parameter rather than dephasing (T_2) due to a distribution of ''static'' local fields commonly observed in a transverse-field measurement. Due to the lack of spin precession, longitudinal-field methods are sensitive to reaction or transition products as well as initial states, provided only that the muon spin polarization is maintained during the change in muonium state. The analysis of longitudinal depolarization curves takes the form

$$A(t) = \sum_i A_0^i G_{LF}^i(t), \qquad (1)$$

where the relaxation functions are $G_{LF}^i(t) = e^{-\lambda_i t}$ as stated above. The vast majority of the data from the current study were satisfactorily fitted using two components: one relaxing due to the charge cycles, and the second from any additional states not participating in the cycle, and therefore having $\lambda = 0$.

The muon spin depolarization due to cyclic muonium charge-state transitions is related to hyperfine oscillations while in the Mu^0 state, together with randomness in the muonium electron's spin orientation for successive periods in the neutral state.[4,2] The effectiveness of each cycle in causing depolarization is controlled by the lifetime of the Mu^0 state compared to the hyperfine period. In essence, the random electron-spin direction is transferred to the muon *via* the hyperfine interaction resulting in the loss of up to half the remaining polarization during each cycle. The net effect is thus proportional to the overall cycle rate, so it depends on the lifetime of the companion state as well as that of the participating Mu^0 center.

In interpreting the interactions responsible for the observed LF depolarization, we have treated the contribution arising from muonium charge-state cycles within the simplest possible model involving two states; one of the two neutral centers and either the Mu$^+$ or Mu$^-$ state.[8] No as-

sumptions have been made as to other transition routes out of either state, thus we have not invoked detailed balance to force any specific relationship between rates for the two transitions. In principle, one can extract the temperature-dependent transition rates along with the Mu^0 hyperfine constant A_{hf} from the temperature and field dependences of the depolarization rates, thereby obtaining a full description of the Mu charge-cycle dynamics. Within the simple two-state model, the field dependence of depolarization rates measured at a constant temperature are typically fit using the approximate expression[4,8]

$$T_1^{-1} \simeq \frac{1}{2}\left(\frac{\lambda_0 \lambda_\pm}{\lambda_0 + \lambda_\pm}\right)\left(\frac{\omega_0^2}{\lambda_0^2 + \omega_{24}^2}\right), \qquad (2)$$

where λ_0 and $\lambda_\pm$ represent the transition rates from Mu^0 $\rightarrow Mu^\pm$ and $Mu^\pm \rightarrow Mu^0$, respectively, while $\omega_0 = 2\pi A_{hf}$ and $\omega_{24} = \omega_0 \sqrt{1 + x^2}$ with $x = B/B_o$ and $B_o = A_{hf}/(\gamma_e + \gamma_\mu)$. Here γ_e and γ_μ are the gyromagnetic ratios for the electron and muon, respectively. This expression yields a curve which is essentially identical to results from a full matrix diagonalization treatment of the complete theory for an *isotropic* center like Mu_T^0.[19] It also works well for anisotropic cases such as Mu_{BC}^0 in the extreme limit of rapid transition rates. In the slow-transition limit the relevant expression becomes much more complicated when the hyperfine interaction is anisotropic.

In practice, our procedure has been to fit constant-temperature $T_1^{-1}(B_{LF})$ curves using Eq. (2) to obtain approximate values for A_{hf} and the two transition rates for a series of temperatures. The hyperfine values identify the appropriate Mu^0 center, since the magnitudes of A_{hf} for Mu_T^0 and Mu_{BC}^0 are vastly different, and the temperature-dependent transition rates yield clues as to the transition processes. We then refit these data in a more global fashion with the hyperfine constants constrained to follow a linear temperature dependence consistent with an extrapolation from low-temperature measurements of A_{hf},[1] and with appropriate temperature-dependent expressions inserted for the transition rates based on initial process assignments. The final fit yields transition rate dynamic parameters for the full set of charge-cycle data. The latter procedure is also more appropriate for fits to constant-field $T_1^{-1}(T)$ curves which make up much of the data from ISIS because of the limited range of magnetic fields available at that facility.

The rate expressions for the various transitions are the least complicated forms consistent with the data and simple models of the relevant processes. These choices, discussed in more detail in our previous work[5] on Mu dynamics in Si, are summarized as follows. Ionizations or activated site changes

$$\lambda_{i(a)} = \nu_o \exp[E_{i(a)}/kT], \qquad (3)$$

carrier capture

$$\lambda_c = n \nu \sigma_c \qquad (4)$$

and combined carrier capture and site changes

$$\lambda_{ac} = n \nu \kappa_{ac} \exp[E_{ac}/kT], \qquad (5)$$

where the final case is labeled as *activated capture*. The various E's represent ionization or activation energies, ν_o is a vibrational prefactor, n and ν are the appropriate temperature-dependent electron or hole densities and velocities, σ_c is the capture cross section, and κ_{ac} is an effective total-process cross section for the combined transition. As will become clear in the discussion, we normally assume that prefactors, energy parameters, and cross sections are independent of temperature, making an exception only when the data clearly dictate otherwise.

We must note here that cyclic ionization/capture transitions might involve either electrons or holes. It is essentially impossible to experimentally distinguish between the two options based on data from a single near-intrinsic sample. Temperature dependences for the capture rates in *n*- or *p*-type samples in the extrinsic region can make such a distinction while doping concentration dependences, which require multiple samples, make a much stronger case for assignment of the specific carrier type. Measurements on doped Ge samples are currently underway to clarify some of the results from the present work which is confined to intrinsic germanium. We did not find any evidence for hole ionization processes for Mu in silicon, and have, in part, used this fact to argue that electrons dominate in Ge as well. However, if the Mu acceptor level lies relatively close to the valence-band edge then hole ionization could be important. Preliminary data on doped samples do show additional h^+ capture processes, but appear consistent with the present process assignments in intrinsic Ge.

The assumptions underlying the treatment outlined above have worked extremely well in describing data on Mu transition dynamics in silicon, and form the starting point for our treatment of muonium transitions in germanium. In silicon we primarily used radio-frequency muon spin resonance (RF-μSR) data to extract transition dynamics and relegated longitudinal depolarization measurements to a qualitative confirmation role; thus far for Ge we have very limited RF-μSR results, and the roles have been reversed, with most of the dynamic information coming from depolarization data.

III. RESULTS AND DISCUSSION

The primary data upon which a model of the charge-state transitions for Mu in germanium has been constructed are displayed in Figs. 1 and 2. Figure 1 shows the field dependence of longitudinal depolarization rates measured at selected constant temperatures. All of these data were obtained at TRIUMF. The time-dependent asymmetry of the muon decay was fit with two components as described in Sec. II: one exponentially relaxing due to the cyclic charge-state transitions, and the second nonrelaxing. The displayed data are the exponential depolarization rate constants obtained for the relaxing component. These curves were initially fit to Eq. (2) with various assumptions regarding the transition processes and the nature of the charge cycle. For 350 K and above, these fits yielded consistent parameters which implied a Mu_T^0 center undergoing ionization and recapture transitions. Although interpreted as e^- processes in a 0/+ charge cycle, identical equations hold if it is a 0/− cycle with h^+ ionization and recapture. When fit individually, the two lower temperature curves (250 and 290 K) yield different
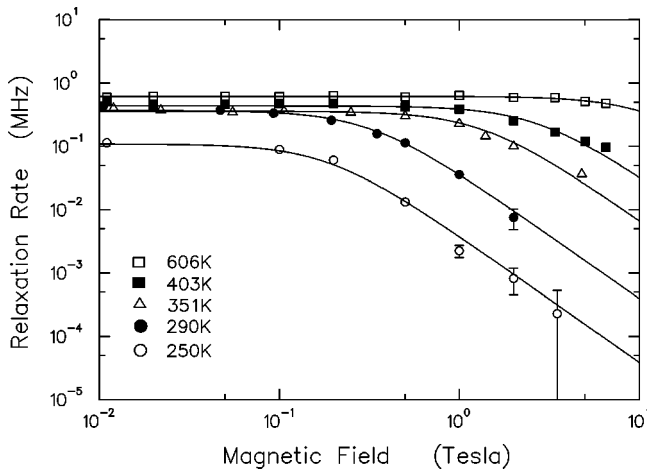
FIG. 1. Longitudinal-field dependence of the muon spin depolarization rates in ultrapure germanium for selected constant temperatures. Data are characteristic of Mu charge cycles involving an isotropic Mu^0 center. The lines represent best fits to Eq. (2.2) with all parameters free.

ionization parameters from the higher-temperature data, and yield better fits assuming a small hyperfine constant consistent with a $0/+$ cycle at the BC site. The slightly different character of these two curves can be seen on close examination of Fig. 1. Although the 290-K curve fits slightly better with the latter assumptions, it could be included in a global fit with the higher-temperature data without significantly altering the parameters. Our criteria for a satisfactory fit include both the χ^2 value and whether the resulting parameters are physically consistent with the process and cycle assumptions. The lines shown in Fig. 1 are from the best free fits to each constant-temperature curve.

Figure 2 shows the temperature dependence of relaxation rate constants obtained at ISIS in low longitudinal (10 mT) and transverse (8 mT) fields. A few higher-temperature
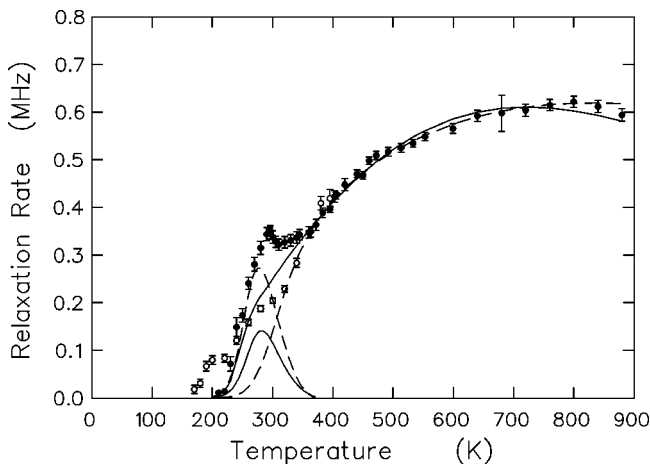
FIG. 2. Temperature dependence of the muon spin depolarization rates for Ge in the low-field limit. Longitudinal-field data (filled symbols) are for $B_{LF}=10$ mT, while transverse-field diamagnetic relaxation rates (open symbols) are for $B_{TF}=8$ mT. Fits imply two separate muonium charge cycles with Mu_T^0 (high temperature) and Mu_{BC}^0 (peak at ~300 K) as the active depolarizing centers. Solid line fits are from LF data only, while dashed fits include TF points for the high-temperature cycle.

transverse-field points were also taken at 2 mT, and were consistent with the longitudinal-field data. The TF curve is from the relaxation rate as observed in the diamagnetic signal and falls below the LF curve for temperatures below roughly 370 K. The overall picture which emerges is of two separate charge cycles which are probed somewhat differently by transverse- and longitudinal-field measurements. Earlier fits[13] to the LF data in Fig. 2 and preliminary fits to the field dependences of Fig. 1 imply that the cycle which dominates the depolarization at higher-temperatures involves Mu_T^0 and the smaller peak centered around 300 K involves Mu_{BC}^0 as the active neutral centers.[13,17] The lines shown in Fig. 2 are based on further fitting as discussed below, and additional experimental checks which confirm this basic picture.

In order to obtain a set of parameters for the cycle involving Mu_T^0 we compared results from separate but correlated fits to the longitudinal-field dependences from Fig. 1 for 350 K and above and to the temperature dependence from Fig. 2 above 370 K. These lower limits are approximately the temperature at which the nonrelaxing component disappears (see later discussion and Fig. 7), implying that all of the muons participate in the same set of depolarizing interactions in the higher-temperature region. Figure 3 shows the hyperfine constants and capture cross sections obtained from fits to the individual curves of Fig. 1 assuming an ionization/capture cycle involving Mu_T^0. As will be discussed in detail, the results of Fig. 3(b) are *effective* cross sections within a two-state, single-cycle model under conditions where the actual dynamics are more complicated. These initial results served as a starting point for additional fits in which the temperature dependences of these two parameters were treated using specific functional forms. The lower-temperature points are included in the figure although those data certainly contain contributions from the second charge cycle. The line in Fig. 3(a) is a linear approximation to the hyperfine variation with ''best-fit'' parameters from a second round of fits over the limited high-temperature region as discussed below. These values are reasonably consistent with an extrapolation of direct hyperfine measurements[20] on Mu_T^0 from below 100 K, included in Fig. 3(a), which yield a $T=0$ hyperfine constant of 2360 MHz.

The capture cross sections [Fig. 3(b)] obtained in the initial fits are temperature dependent, and 2–3 orders of magnitude smaller than expected for e^- capture by a positively charged center (or h^+ by a negative one). The neutral center in this cycle is Mu_T^0, while the positive state is in the other configuration, Mu_{BC}^+, based on theoretical results;[9] thus activated capture might be anticipated. When fit as activated capture the barrier is negative (-67 meV), generally consistent with the decrease in cross section with temperature as displayed in Fig. 3(b). This explanation is not very satisfactory, nor is the alternative of a $0/-$ cycle with the muon staying at the T site and hole ionization and recapture, which should certainly have larger (Coulombic) cross sections. All other cycle and process assignments that were tried gave at least one parameter which was far outside physically acceptable bounds. Specifically, other likely process assignments for a T site $0/-$ cycle, e^- capture and ionization or alternating e^- and h^+ capture, resulted in very poor fits even with
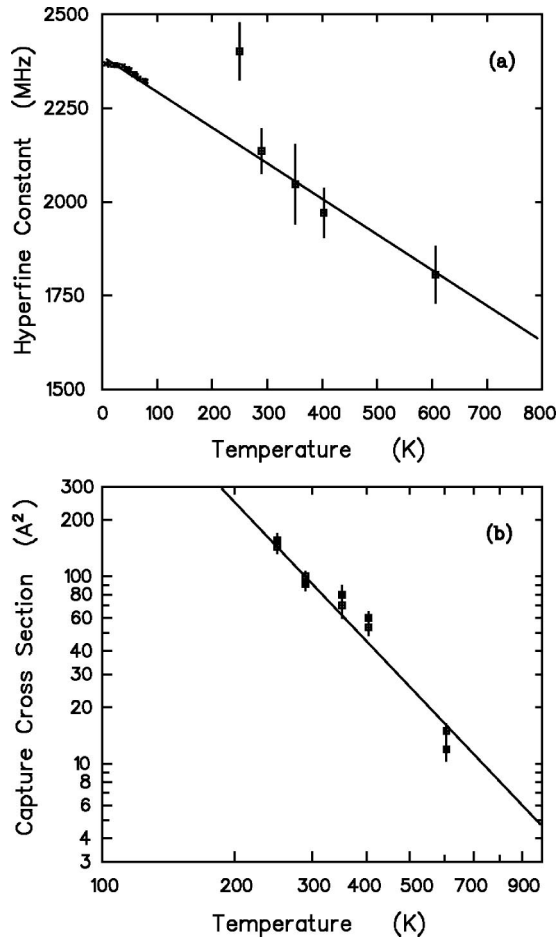
FIG. 3. (a) Hyperfine constants and (b) effective capture cross sections obtained from free fits to the data of Fig. 1 under assumptions of an e^- ionization and a recapture charge cycle involving Mu_T^0. The lowest-temperature curve fits better assuming Mu_{BC}^0. Lines represent best-fit temperature dependences from subsequent constrained fits. See the text for details. Hyperfine data below 100 K in (a) are direct measurements from Holzschuh (Ref. 20).

temperature-dependent parameters unless the hyperfine constant was allowed to become much larger than that for vacuum, Mu^0. Based on this preliminary analysis we therefore assigned the high-temperature data to a $Mu_T^0 \rightleftharpoons Mu_{BC}^+ + e^-$ cycle. We will return to a discussion of this result and a series of experimental checks below. In subsequent fits, the capture half of the cycle was somewhat arbitrarily described using a power law to account for the temperature-dependent cross sections since it worked better empirically than an exponential function. Based on Fig. 3(b), which shows results from two preliminary fits to the curves in Fig. 1 with A_{hf} either free (filled symbols) or confined to the linear dependence from Fig. 3(a) (open symbols), a functional form of $\sigma = \sigma_o T^{-2}$ was assigned to the cross sections. With the exponent free, fits to the data of Fig. 2 are consistent with this choice.

Using the specific choices of functional forms for the cross sections and hyperfine parameters described above, separate constrained fits were performed on the data from Figs. 1 and 2 over the restricted temperature range of ~ 350 K and above. Because of the strong correlations between the hyperfine and capture parameters observed in ini-

tial attempts, we choose to quote transition rate parameters obtained with fixed hyperfine parameters. The ''best'' hyperfine parameters were selected by optimizing agreement between the transition parameters obtained from a fit to the three higher-temperature field-dependence curves (Fig. 1) with those obtained from the low-field temperature dependence (Fig. 2). The most consistent results were obtained with hyperfine constants (in MHz) of $A_{hf} = 2385 - 0.92$ T giving averaged transition parameters of $\nu_o = (6.7 \pm 0.8) \times 10^7$ MHz, $E_i = 167.1 \pm 1.5$ meV, and $\sigma_o = (7.8 \pm 0.9) \times 10^6$ Å^2 K^2 with values for the two separate results falling within the quoted error bars. Variations in A_{hf}^o and dA/dT of roughly ± 40 MHz and ± 0.05 MHz/K, respectively, resulted in similar χ^2 values but with somewhat larger differences in transition parameters from the two data sets. In all cases, the ionization energy remained within 168 ± 4 meV, with the prefactor and cross section parameter varying over considerably wider ranges. The solid lines in Fig. 2 and those for the parameter variations in Fig. 3 represent the end results based on this procedure.

As a final check on our characterization of the high-temperature cycle, we note that the above fit falls slightly above the TF data in Fig. 2 down to the shoulder near 300 K. Since Mu_T^0 is much more efficient than Mu_{BC}^0 in the charge-cycle depolarization process, we consider the possibility that the TF relaxation rates T_2^{-1} above roughly 315 K may be dominated by T_1^{-1} from the high-temperature cycle and include those TF rates in an expanded trial data set for the Mu_T^0 cycle. A fit to this expanded set, with all parameters free, yields the following results. The hyperfine constant is $A_{hf} = (2453.8 \pm 2.8) + (0.659 \pm 0.089)$ T, and the corresponding ionization parameters are $\nu_o = (1.16 \pm .42) \times 10^7$ MHz and $E_i = 174.8 \pm 1.2$ meV, and the capture cross-section parameter is $\sigma_o = (1.34 \pm 0.45) \times 10^5$ Å^2 K^2. This alternative procedure forms the basis for the cycle separation which leads to the dashed curves in Fig. 2. Fits to the three higher-temperature longitudinal field-dependent curves alone with the hyperfine constants fixed to this result give transition parameters more consistent with those previously listed. The basic conclusion from this attempt to extend the range of data describing the high-temperature cycle is that the included transverse-field rates should be considered as a lower limit on Mu_T^0 charge-cycle depolarization rates in the region where both cycles contribute.

In order to obtain an estimate for the parameters characterizing the transition dynamics associated with the longitudinal depolarization peak near 300 K, the rates resulting from the fits to the high-temperature region were subtracted from the experimental rates shown in Fig. 2. The difference was then treated as the contribution from a second two-state charge cycle and fitted to Eq. (2) as before. This estimate for the second contribution obviously depends critically on extrapolation below the ~ 350-K lower limit used in analysis of the high-temperature longitudinal data, thus we report results with and without the TF rates included. In either case this procedure yields reasonable parameters for a 0/+ cycle at the BC site which are generally consistent with results from the 250-K field dependence where this second cycle dominates the depolarization. Using the ''free'' fit to the combined LF and TF temperature dependence just discussed

yields a Mu_{BC}^0 ionization energy of 215 ± 10 meV with a prefactor of $(2.1\pm0.7)\times10^7$ MHz, and a capture cross section of 2488 ± 19 Å^2 along with an effective hyperfine constant of 25–28 MHz near the peak, roughly equal to the low temperature value of $A_\parallel=27.3$ MHz for Mu_{BC}^0.[1] Given the complications of the data separation and theoretical complexity for an anisotropic Mu^0 center, these hyperfine values fully justify the assignment of a cycle involving Mu_{BC}^0, but should be accorded no additional significance. The dashed result for the lower-temperature peak in Fig. 2 is from this particular fit. When using the parameters obtained by optimizing the consistency between fits to the TRIUMF and ISIS longitudinal-field data as the basis for subtraction of the Mu_T^0 contribution, we obtain a slightly higher Mu_{BC}^0 ionization energy of 229 ± 18 meV with a prefactor near 3×10^7 MHz and a capture cross section of about 2550 Å^2 when using temperature-dependent hyperfine parameters appropriate to Mu_{BC}^0. The uncertainties in prefactor and capture cross section were large, as were the variations with slightly different choices for the BC hyperfine constants. This separation of the two cycles is represented by the solid-line fits in Fig. 2 as stated previously. In either of these procedures the Mu_{BC}^0 hyperfine interaction was treated as an effective isotropic average. The uncertainties in separating contributions from the two cycles do not warrant dealing with the computational difficulties of properly including the anisotropy. We checked that our data separation procedures did not introduce major inconsistencies by extrapolating results for the BC cycle to high temperatures, and found that its maximum contribution to the depolarization above 350 K was only a few percent of the measured rates.

Overall, fits with slightly different constraints have been quite consistent for the ionization steps of both cycles, but much less stable regarding capture parameters. There are fairly large correlations between the hyperfine constants and capture cross sections. The available data will not support a simultaneous fit to both cycles. They in fact just barely allow free fits to just one cycle, thus we have presented results based on making specific choices for the hyperfine parameters in regions where direct measurements do not exist by requiring consistency with extrapolations from below 100 K and with our initial free-parameter fit results. The accompanying table represents our present best estimate of rate parameters for Mu transitions in germanium.

We briefly return to questions regarding identification of the charged Mu center in the cycle involving Mu_T^0 and the temperature-dependent capture cross sections for that cycle. The decrease in effective capture cross section with increasing temperature is unexpected. In other cases we have observed constant cross sections with the only temperature dependence occurring in n and v. A plausible explanation arises if we consider the high-temperature effects from a BC cycle with e^- as the active carrier. First, if the two cycles were completely independent, such as for $Mu_T^0 \rightleftharpoons Mu_T^- + h^+$ and $Mu_{BC}^0 \rightleftharpoons Mu_{BC}^+ + e^-$, one expects similar capture cross sections typical of Coulomb capture by a charged center, on the order of a few thousand Å^2. Such a result is obtained for the BC case but not for the T-site cycle. Other options for an independent T-site cycle, such as $Mu_T^- \rightleftharpoons Mu_T^0 + e^-$ or alternating h^+ and e^- capture by Mu_T, were ruled out because

unreasonably large hyperfine constants were necessary to obtain decent fits, as previously mentioned. Thus the most consistent analysis of our data appears to indicate that the two Mu^0 centers remain in their respective sites throughout their lifetimes, but both are communicating with a common Mu^+ state via e^- ionization and recapture. Because of the vastly different hyperfine interactions the effect of these cycles on the muon polarization is quite different. The maximum effect from Mu_{BC}^0 occurs for much slower cycle rates and is thus considerably weaker than that from Mu_T^0. Once the cycle through the BC neutral becomes rapid compared to the Mu_{BC}^0 hyperfine frequency, its effect on the depolarization becomes negligible, as indicated in the previous paragraph. However, the BC cycle continues to occur, and thus reduces the net time available for capture into the competing cycle through Mu_T^0. The BC capture rate increases more rapidly than the ionization rate based on the fitted parameters. Therefore a greater fraction of time is spent in the Mu_{BC}^0 state as the temperature increases, thereby reducing access to the Mu_T^0 cycle. The fact that the muon must change site to enter the Mu_T^0 state in addition to capturing an electron contributes to making that capture route a less favorable option. This combination of factors and the cycle assignments are at least consistent with a reduced effective capture rate into Mu_T^0 at higher temperatures. We have been unsuccessful in constructing a similar qualitative explanation for unexpected parameter values associated with any of the alternative charge-cycle assignments.

A more thorough theoretical understanding of the details of the capture processes and the associated site change needs to be developed before a more realistic model of the effective capture dynamics can be constructed. When the high-temperature data are fit within a simple two-state model, the capture parameters apparently adjust to account for the second charge cycle which has little or no direct effect on the muon depolarization, while the hyperfine and ionization parameters which primarily control the depolarization are well determined. With respect to process assignments, as the temperature increases hole capture may contribute along with electron ionization as a $Mu^0 \rightarrow Mu^+$ transition process. Measurements on p-type Ge samples where h^+ capture occurs at low temperatures are required to obtain the relevant cross sections so that rates for the two routes can be compared. Even within a cycle which involves just two states, a missing transition route may lead to odd parameter values, and thus could also contribute to the observed cross-section behavior.

Our results for cyclic muonium charge-state transitions, particularly the ionization parameters, can be compared to previous studies of Mu transitions in Ge. Both the Mu_{BC}^0 and Mu_T^0 transverse-field μSR signals broaden and disappear near 100 K,[1] and the reappearance of these fractions in the diamagnetic TF-μSR signal occur at higher temperatures.[1] The growth of the diamagnetic fraction between 160 and 300 K in n-type Ge was treated previously[16] as an ionization from Mu_T^0 to Mu_{BC}^+, although neither site was yet established at that time. The energy parameters from that work agree very closely with the values we obtain from the high-temperature charge cycle involving Mu_T^0, so that we can be quite confident of this assignment and ionization energy.

In light of the ionization energies obtained in the present

work, the nature of the disappearance of the two Mu^0 TF-μSR precession signals near 100 K needs to be reassessed. We have used a combination of literature data[15,21–24] for this purpose, and obtained the following activation energies and prefactors: 18.8 ± 2.0 meV and ~81 MHz for the disappearance of the Mu_T^0 precession signal and similar low values of 30.3 ± 4.5 meV and ~48 MHz for Mu_{BC}^0. These results compare well with energies of 12–14 and 26 meV originally obtained from a subset of these data,[1,15,21] but are inconsistent with the charge-cycle ionization energies. We conclude that the low-temperature disappearance of the Mu_T^0 and Mu_{BC}^0 precession signals is not due to ionization, and suggest instead that it results from the onset of bidirectional site transitions for Mu^0. By implication, in Ge both the T and BC sites are visited in the course of diffusion of neutral muonium below ~150 K. This contrasts with results[5] in Si where any low-temperature site changes are strongly coupled to charge-state transitions.

Theoretical calculations[14] find that the local minima in total energy for the two Mu^0 configurations are at nearly the same depth in Ge, suggesting that the T site lies slightly deeper than the BC site. Based on the site-change assignment for the low-temperature Mu^0 transitions, we conclude that the potential energy surface for Mu^0 must be much flatter in Ge than in Si. The very small difference in barrier heights confirms that the two Mu^0 centers have nearly identical energies in Ge; however, the data indicate that Mu_{BC}^0 remains the more stable center just as in Si. These fits further imply that the site transitions are initiated by a low-frequency interaction, such as with acoustic phonons, rather than by the optical-phonon interaction which apparently triggers the T to BC site transitions in silicon and diamond.[25]

Several measurements can be performed to seek additional evidence supporting low-temperature Mu^0 site changes. Bidirectional site changes will switch the hyperfine constant between very different values, causing muon depolarization in a longitudinal field. We therefore performed low-temperature longitudinal depolarization measurements with the results shown in Fig. 4. At 10 mT a $\sim40\%$ relaxing fraction is observed at low temperatures along with a missing fraction of about the same size and a nonrelaxing component of slightly above 12%. The various components are temperature dependent, and the relaxation does not match the characteristics expected from motion of Mu_T^0, but rather appears to imply slow transitions involving that state. The field dependence at 75 K (not shown) indicates that the relaxing component is associated with Mu_T^0. We have fit the relaxing amplitude with a simple model for bidirectional transitions without attempting to model the relaxation rates in detail. The line in Fig. 4(b) represents this fit which yielded barriers of roughly 25 and 55 meV, with Mu_{BC}^0 representing the lower-energy state. Because of simplifications in the model, these energies are only approximate; however, these results are consistent with assignment of slow Mu^0 site changes to the low-temperature transitions, and confirm the general characteristics derived from the TF-μSR data. Several additional qualitative checks have shown nothing which is incompatible with this assignment.

For completeness, we include the TF-μSR data on the diamagnetic state in the same germanium sample. Figure 5
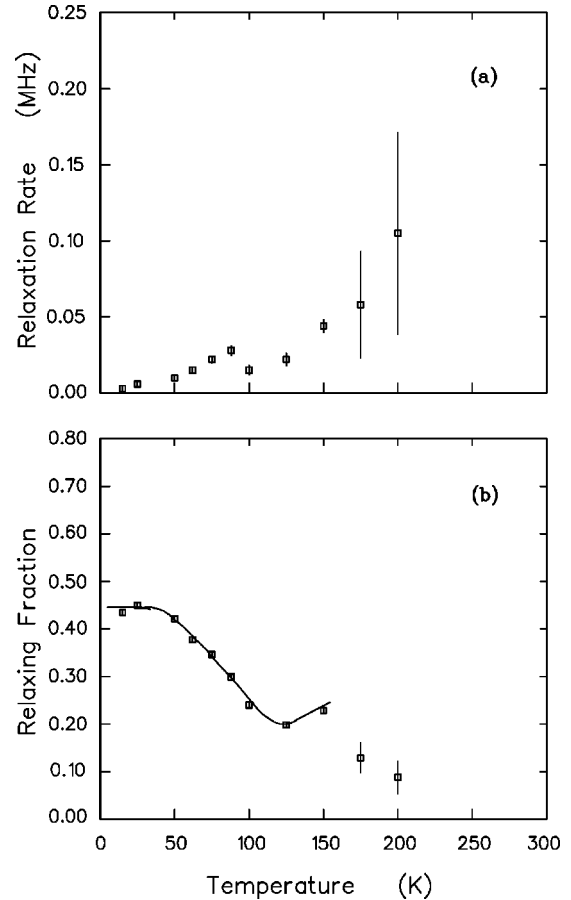
FIG. 4. The low-temperature longitudinal-field relaxation data for Mu in Ge: (a) relaxation rate and (b) relaxing fraction versus temperature below the onset of charge cycles. The curve in (b) is from a simplified model of Mu^0 site transitions.

shows the amplitude, relaxation rate, and phase for the diamagnetic precession signal at 8 mT. This signal can be due to either Mu^+ or Mu^- as well as any diamagnetic Mu complex such as a Mu-impurity pair. The visible signal in these transverse-field measurements represents only diamagnetic states formed rapidly compared to the precession frequency of any precursor state because of the phase coherence requirements. The primary features associated with transition dynamics in these data are step increases in the amplitude as a function of temperature and dips in the phase, both of which imply transitions into one of the diamagnetic Mu states. In the displayed data, the rise in relaxation rate starting at 220 K is associated with the charge cycles; these data were included in Fig. 1 along with the longitudinal-field depolarization rates. The largest dip in phase, peaking near 180 K and the rise in amplitude between 150 and 200 K coincide with the ionization of one or both of the Mu^0 centers. The weaker feature in the phase and a very small step in amplitude occurring near 100 K may be related to the Mu^0 site transitions, and would be consistent with one of the Mu^0 states being a precursor to a slowly formed bound Mu state, most likely to occur when the highly mobile Mu_T^0 center encounters some specific impurity. As discussed below, the phase feature at very low temperatures may be from a similar process.

Other evidence exists for strong interactions of muonium
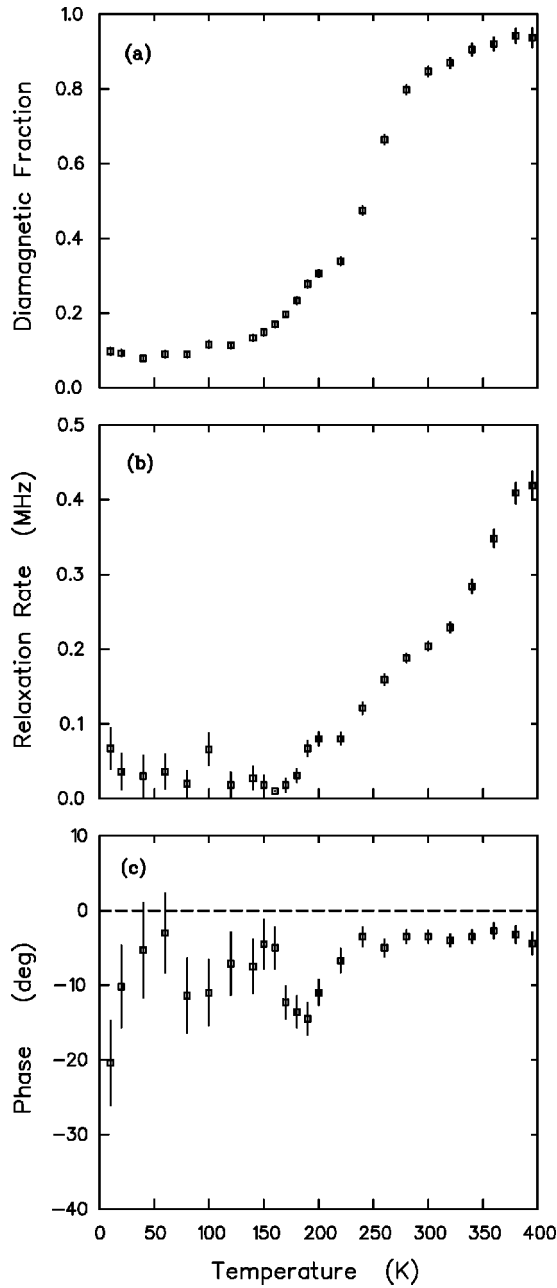
FIG. 5. Transverse-field μSR precession data for the diamagnetic Mu states in Ge: (a) diamagnetic amplitude, (b) relaxation rate, and (c) phase as a function of temperature.

with impurities in germanium. TF-μSR data on Mu_T^0 in doped Ge, specifically n-type samples[15] below the donor ionization temperature ($T < 20$ K) and samples doped with isovalent Si,[22] show strong interactions of the mobile neutral center with impurity atoms. We interpret these relaxation data as evidence for charge-transfer interactions of the type

$$Mu_T^0 + I^0 \rightarrow Mu_T^- + I^+, \tag{6}$$
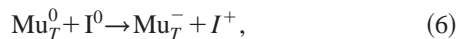
where this particular polarity for the charge transfer is appropriate for donor impurities. The ionized product states will be strongly attracted to each other and may form a bound pair [Mu,I]. The phase feature at very low temperatures in Fig. 5(c) likely arises from interactions of this type, as do low-temperature Mu_T^0 relaxation rates which are proportional
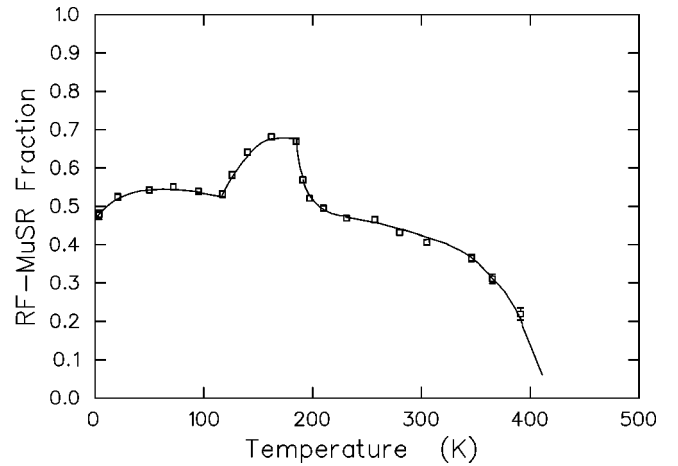
FIG. 6. RF-μSR data for Ge. The normalized time-integral diamagnetic intensity as a function of temperature. The line is intended as a guide to the eye. Comparison with Fig. 5(a) implies a diamagnetic state slowly formed at low temperatures and persisting to near 400 K.

to I^0 concentrations.[15] Our RF-μSR data on the present Ge sample show a time-integrated diamagnetic fraction above 50% at low temperatures (TRIUMF data, Fig. 6) compared to about a 10% fraction visible in the TF-μSR precession measurements [Fig. 5(a)]. The combination of these results implies a slowly formed diamagnetic Mu state even at the very lowest temperatures. The increase in the diamagnetic fraction in the RF data between 100 and 200 K is related either to ionization yielding Mu^+, or to the site-change transitions for Mu^0 which cycle more muons through the mobile T site species and the associated increase in interactions with impurities. The decrease near 200 K is a signal of the onset of charge cycles. The RF data imply that the slowly formed diamagnetic state remains a significant fraction until about 400 K at which point it dies out quickly. From the data discussed thus far, this state could either be an isolated Mu_T^- or a bound [Mu,I] pair. Optical excitation measurements[26] on n-type Ge imply a slowly formed diamagnetic state with a level outside the band gap, consistent with formation of a [Mu,donor] pair.

The final piece of evidence related to a bound Mu state comes from the nonrelaxing fraction observed in our longitudinal depolarization measurements. In the charge-exchange regime this second signal represents a muon in some diamagnetic state which is not participating in the charge cycles. The temperature dependence of the nonrelaxing fraction is shown in Fig. 7 over the temperature region where this signal disappears. We have fit the disappearance to an activated process, initially assuming Mu_T^- ionization, and obtained an energy parameter of 0.748 ± 0.012 eV. This energy is in fact larger than the Ge band gap in this temperature region (0.655 eV at 350 K), and therefore cannot be assigned to thermal ionization of Mu_T^-. This leaves a bound [Mu,I] pair as the most plausible assignment, in which case the energy parameter is for pair dissociation. Based on the reported impurity content, C, Si, and O are by far the highest concentration contaminants. Carbon is known to form clusters in Ge and does not provide a large concentration of isolated defects. Both O and Si are strong candidates; oxygen easily forms
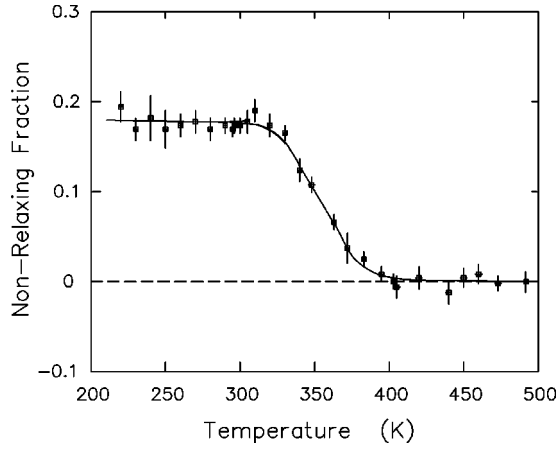
FIG. 7. The nonrelaxing amplitude vs temperature from longitudinal relaxation measurements on Ge in the charge-cycle regime. This signal is identified as a bound-Mu complex. The fitted curve yields a dissociation energy of 0.75 eV.

FIG. 8. Summary of temperature-dependent rates for transitions between isolated muonium centers in ultrapure Ge based on the present work. The charge-state transitions are identified as e^- ionization and capture processes; the transition rate parameters are listed in Table I.

O-H bonds in many situations, and silicon is known to strongly interact with Mu_T^0 in Ge, causing low-temperature relaxation which could indicate pair formation.[22] Because of the demonstrated interaction of silicon impurities with the mobile Mu_T^0 center, we suspect that the observed state is a bound [Si,Mu] pair, but cannot make a firm identification.

Finally, in order to check for overall consistency of the model of Mu transition dynamics which emerges from the present work, we compare the relative transition rates which result from our process assignments and the associated dynamic parameters as summarized in Table I. Figure 8 displays all of the transition rates obtained for isolated muonium states in intrinsic Ge as a function of temperature. First of all, we see that above approximately 220 K the slowest transitions of this set are the Mu^0 site changes, because of their low prefactors. Therefore, in the region where the charge cycles are active the fitted ionization rates are much more rapid than the site transitions, fully consistent with the physical picture of separate relaxation peaks due to Mu_T^0 and Mu_{BC}^0. Furthermore, it becomes apparent that the charge cycles are initiated by rapid growth of the electron-capture rates in the intrinsic case represented by this ultrapure Ge sample. The capture rates into Mu_T^0 reach the site-change rates roughly 30–50 K higher than does capture into Mu_{BC}^0,

consistent with the fits in Fig. 2. In heavily doped n-type samples where the electron capture rates are controlled by the extrinsic e^- concentrations, one would expect these charge cycles to become active at lower temperatures where the ionizations become rapid. Additionally, at higher donor concentrations there would likely be e^- capture by Mu_T^0 to form the Mu_T^- state, which we do not observe in the present sample, and the possibility of a $0/-$ cycle at the T site which would become active when Mu_T^- ionizes.

Returning to the present situation, there are three additional crossover points observed in Fig. 8 where one might expect to see changes in dynamic features, particularly the measured depolarization rates. One of these is at 118 K where the ionization becomes faster than the site change for Mu_T^0. Examining the various experimental data sets, the increase in RF-μSR diamagnetic fraction occurs at roughly 120 K (Fig. 6), there is a discontinuity in the LF relaxation rates near 100 K [Fig. 4(a)], and small features may be present in the TF parameters near 100 K (Fig. 5). While it is difficult to say for sure whether any of these specifically result from ionization or are simply related to the site changes, at least the RF feature appears to be well correlated with this rate crossover. The second point is at roughly 160

TABLE I. Transitions identified for muonium in germanuim along with current best estimates for the parameters describing the transition dynamics.

Mu transition	Rate parameters		
Charge transitions for Mu_{BC}^0:			
$Mu_{BC}^0 \rightarrow Mu_{BC}^+ + e^-$	$\nu_{BC}^{0/+} = 2.9 \times 10^7$ MHz	$E_{BC}^{0/+} = 229 \pm 18$ meV	
$Mu_{BC}^+ + e^- \rightarrow Mu_{BC}^0$	$\sigma_{BC}^{+/0} = 2550 \pm 400$ Å^2		
Charge transitions for Mu_T^0:			
$Mu_T^0 \rightarrow Mu_{BC}^+ + e^-$	$\nu_{T/BC}^{0/+} = 6.7 \times 10^7$ MHz	$E_{T/BC}^{0/+} = 167.1 \pm 1.5$ meV	
$Mu_{BC}^+ + e^- \rightarrow Mu_T^0$	$[\sigma_{BC/T}^{+/0} = 7.8 \times 10^6 T^{-2}$ Å$^2]^a$		
Site transitions:			
$Mu_T^0 \rightarrow Mu_{BC}^0$	$\nu_{T/BC}^0 = 81$ MHz	$E_{T/BC}^0 = 18.8 \pm 2.0$ meV	
$Mu_{BC}^0 \rightarrow Mu_T^0$	$\nu_{BC/T}^0 = 48$ MHz	$E_{BC/T}^0 = 30.3 \pm 4.5$ meV	

^{a}Effective cross section when data are fit to a two-state, single-charge-cycle model.

K, where the Mu_{BC}^0 ionization becomes faster than the site change. This temperature corresponds to the onset of growth of the TF-μSR (Fig. 5) amplitude and a major dip in phase, implying a transition into a diamagnetic state, thereby identifying these features with ionization transitions. The third point is just below 400 K where the extracted rate for e^- capture to form Mu_{BC}^0 exceeds the Mu_{BC}^0 ionization rate. This is especially interesting as it relates to our argument regarding the reduced capture rates for the competing channel into Mu_T^0. Above this crossover the fitted rates imply that more time is spent as Mu^0 than as Mu^+ in the charge cycle for which the muon stays at the bond-centered location. Overall, we find that the total picture presented here is internally consistent. Furthermore, we have not found any other data which rule out any part of this picture. Thus we are reasonably confident that the major assignments within this model are basically correct. A portion of the Mu dynamics in Ge which is definitely missing are the various hole processes. Adding the hole-related transitions as well as those involving Mu^- mentioned above must await results on doped Ge samples. Such data will also serve as a fairly stringent test of a number of the present process assignments.

IV. CONCLUSIONS

In conclusion, we have used the measured longitudinal depolarization rates in an ultrapure Ge sample to extract the ionization and electron capture dynamics associated with rapid cyclic muonium charge-state transitions. Two separate charge cycles are found for Mu in germanium, one involving the Mu_T^0 center and the second involving Mu_{BC}^0. In both cases the data are best fit assuming a 0/+ charge cycle with electron ionization and recapture as the transition processes. The implication is that both neutral centers communicate with a common Mu_{BC}^+ state during the cyclic exchange of electrons with the conduction band. The resulting ionization energies are approximately 0.17 and 0.23 eV, respectively, for the T and BC configurations. Both of these energies are much larger than the activation energies obtained previously for the low-temperature disappearance of the TF-μSR precession signals from Mu_T^0 and Mu_{BC}^0. The 100 K transitions out of these states have consequently been reassigned to bidirectional site changes for Mu^0. With this assignment, we determine that the BC configuration is slightly (~ 12 meV from previous TF-μSR data) more stable than the T site for Mu^0 in germanium, and that the barrier and prefactors are very small for Mu^0 site changes. The resulting model of transitions among isolated Mu states in Ge appears to be internally consistent, and satisfactorily explains numerous experimental features in intrinsic Ge. Further tests on Mu transitions in doped samples are required to verify process assignments and to add the Mu^- state and hole processes in order to obtain a complete picture of muonium dynamics in germanium. We find evidence of a bound Mu state, tentatively assigned to a [Si,Mu] pair, which is slowly formed from a mobile Mu_T^0 precursor and has a binding energy of 0.75 eV.

[1] B.D. Patterson, Rev. Mod. Phys. **60**, 69 (1988).

[2] K. H. Chow, B. Hitti, and R. F. Kiefl, in *Identification of Defects in Semiconductors*, edited by M. Stavola (Academic Press, New York, 1998), p. 137.

[3] R. F. Kiefl and T. L. Estle, in *Hydrogen in Semiconductors*, edited by J. Pankove and N. M. Johnson (Academic Press, New York, 1991), p. 547.

[4] K.H. Chow, R.F. Kiefl, J.W. Schneider, B. Hitti, T.L. Estle, R.L. Lichti, and C. Schwab, Phys. Rev. B **47**, 16 004 (1993).

[5] S.R. Kreitzman, B. Hitti, R.L. Lichti, T.L. Estle, and K.H. Chow, Phys. Rev. B **51**, 13 117 (1995).

[6] B. Hitti, S.R. Kreitzman, T.L. Estle, E.S. Bates, M.R. Dawdy, T.L. Head, and R.L. Lichti, Phys. Rev. B **59**, 4918 (1999).

[7] K.H. Chow, R.F. Kiefl, W.A. MacFarlane, J.W. Schneider, D.W. Cooke, M. Leon, M.A. Paciotti, T.L. Estle, B. Hitti, R.L. Lichti, S.F.J. Cox, C. Schwab, E.A. Davis, A. Morrobel-Sosa, and L. Zavich, Phys. Rev. B **51**, 14 762 (1995).

[8] K.H. Chow, B. Hitti, R.F. Kiefl, S.R. Dunsiger, R.L. Lichti, and T.L. Estle, Phys. Rev. Lett. **76**, 3790 (1996).

[9] S.K. Estreicher, Mater. Sci. Eng., R. **14**, 319 (1995).

[10] R. Kadono, R.F. Kiefl, J.H. Brewer, G.M. Luke, T. Pfiz, T.M. Riseman, and B.J. Sternlieb, Hyperfine Interact. **64**, 635 (1990).

[11] T.L. Estle, K.H. Chow, S.F.J. Cox, E.A. Davis, B. Hitti, R.F. Kiefl, R.L. Lichti, and C. Schwab, Mater. Sci. Forum **258-263**, 849 (1997).

[12] R.L. Lichti, C. Schwab, and T.L. Estle, Mater. Sci. Forum **196-201**, 831 (1995).

[13] R.L. Lichti, K.H. Chow, D.W. Cooke, S.F.J. Cox, E.A. Davis, R.C. DuVarney, T.L. Estle, B. Hitti, S.R. Kreitzman, R. Macrae, C. Schwab, and A. Singh, Hyperfine Interact. **86**, 711 (1994).

[14] S.K. Estreicher and Dj.M. Maric, Phys. Rev. Lett. **70**, 3963 (1993).

[15] A. Weidinger, G. Balzer, H. Graf, E. Recknagel, and Th. Wichert, Phys. Rev. B **24**, 6185 (1981).

[16] D.G. Andrianov, G.G. Myasishcheva, Yu.V. Obukhov, V.S. Roganov, G.I. Savel'ev, V.G. Firsov, and V.I. Fistul', Fiz. Tekh. Poluprovodn. **12**, 161 (1978) [Sov. Phys. Semicond. **12**, 92 (1978)].

[17] R.L. Lichti, K.H. Chow, S.F.J. Cox, T.L. Estle, B. Hitti, and C. Schwab, Mater. Sci. Forum **258-263**, 179 (1997).

[18] K.H. Chow, R.L. Lichti, R.F. Kiefl, S. Dunsiger, T.L. Estle, B. Hitti, R. Kadono, W.A. MacFarlane, J.W. Schneider, D. Schumann, and M. Shelley, Phys. Rev. B **50**, 8918 (1994).

[19] K. H. Chow, Ph.D. dissertation, University of British Columbia, 1995.

[20] E. Holzschuh, Phys. Rev. B **27**, 102 (1983).

[21] E. Holzschuh, H. Graf, E. Recknagel, A. Weidinger, and Th. Wichert, Phys. Rev. B **20**, 4391 (1979).

[22] K.P. Döring, N. Haas, E.E. Haller, D. Herlach, W. Jacobs, M. Krauth, H. Orth, J. Rosenkranz, A. Seeger, J. Vetter, K.P. Arnold, Th. Aurenz, and H. Bossy, Physica B **116**, 354 (1983).

[23] K.W. Blazey, T.L. Estle, E. Holzschuh, W. Odermatt, and B.D. Patterson, Phys. Rev. B **27**, 15 (1983).

[24] C.W. Clawson, E.E. Haller, K.M. Crowe, S.S. Rosenblum, and J.H. Brewer, Hyperfine Interact. **8**, 417 (1981).

[25] T.L. Estle and R.L. Lichti, Hyperfine Interact. **97-98**, 171 (1996).

[26] R. Kadono, R.M. Macrae, K. Nagamine, and K. Nishiyama, Hyperfine Interact. **105**, 303 (1997).